

# QUARZ-CSP

## Test- und Evaluationszentrum

### Messungen der Reflektivität von optischen Komponenten für konzentrierende Solartechnik

Measurement of reflectivity of optical components for  
concentrating solar power technology

### Test Report

Alanod Order No. 514838

DLR KTr 3001588

Messung von Reflektivität und Strahlaufweitung an Miro und Miro-Sun Proben

Stephanie Meyen  
Eckhard Lüpfer

DOC: Quarz-Reflex\_0905\_Alanod

**Auftraggeber/Client: Alanod**

Deutsches Zentrum für Luft- und Raumfahrt  
German Aerospace Center  
Institute of Technical Thermodynamics – Solar Research  
51147 Köln, Germany  
Tel. +49 2203 601 3214  
Email: [stephanie.meyen@dlr.de](mailto:stephanie.meyen@dlr.de); [eckhard.luepfert@dlr.de](mailto:eckhard.luepfert@dlr.de)

08.05.2009



## Contents

1. Description .....	3
2. Results .....	4
2.1. Averaged reflectance spectra.....	4
2.2. Calculated results .....	9
2.3. Images of specular beam diversion .....	12
3. Summary and evaluation.....	14

## 1. Description

Ten aluminum mirror samples have been provided by Alanod for optical testing. These were ca. A4-sized sheets of 0.5 mm thickness of the following materials:

1 x 4270 GP (Mi); commercially: MIRO

3 x 4270 GP + N-Lack (Rd1 / Mi / Rd2); commercially: MIRO-Sun

3 x 4270 GPNV + B-Lack (Rd1 / Mi / Rd2); commercially: MIRO-Sun

3 x 4270 GPNV + K-Lack (Rd1 / Mi / Rd2); commercially: MIRO-Sun

Spectral reflectivity measurements have been performed on the samples of each material with a *Perkin-Elmer Lambda 950* spectrometer at 8° incidence angle. For the spectral hemispherical reflectance  $\rho_{\text{hem},\lambda}$  the instrument was equipped with an *integrating sphere accessory* (150 mm diameter) and a NIST-traceable mirror standard was used as reference. Every sample was measured in 4 positions, rotated each time by 90° in the sample port. The average and standard deviation of the four measurements was used for further evaluation. The measurements took place in the wavelength range 250nm – 2500nm in 5nm intervals.

With a *universal reflectance accessory* (URA) the spectral specular reflectance  $\rho_{\text{spec},\lambda}$  was also measured in the same wavelength range. Here absolute measurements of the samples were taken in three positions, each time rotated by 45°. The average and standard deviation of the three measurements was used for further evaluation.

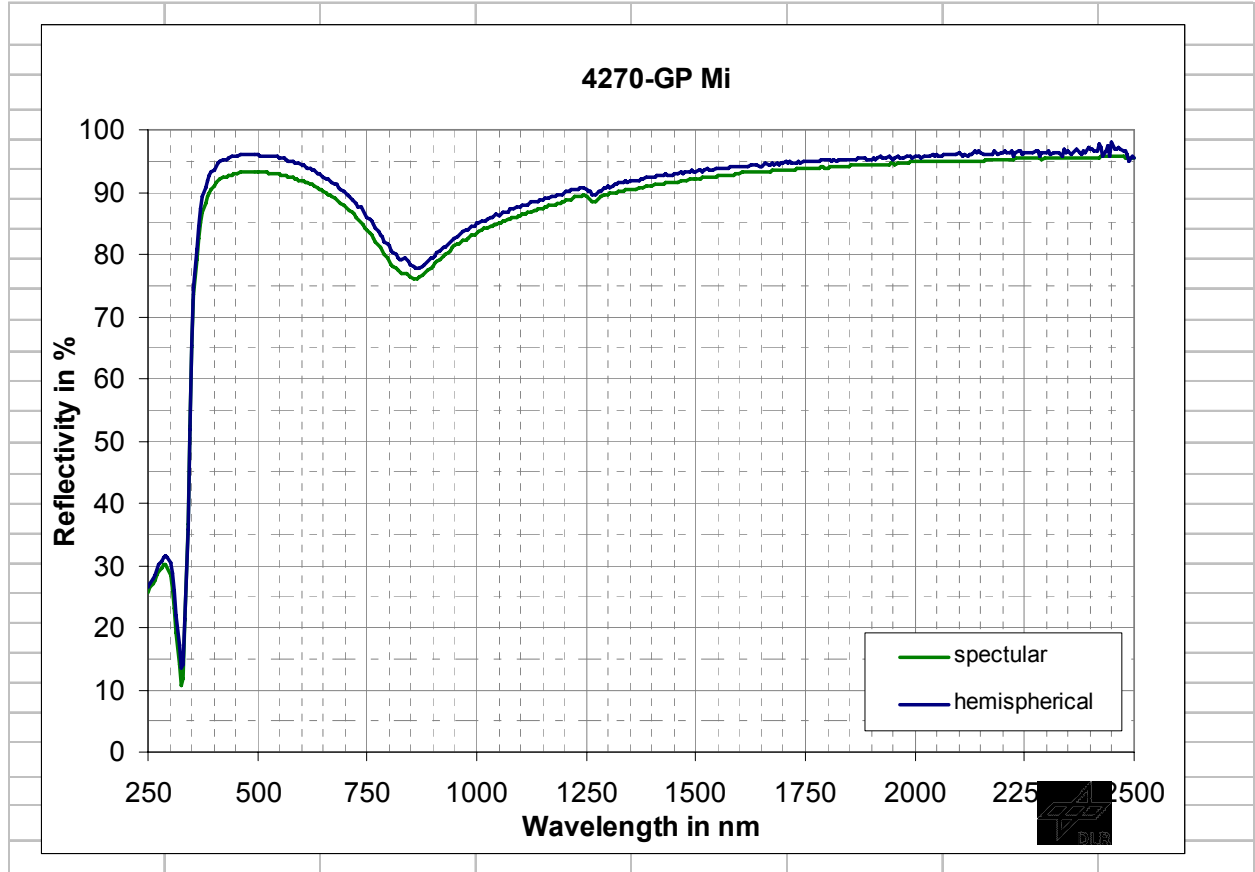
The results of  $\rho_{\text{hem},\lambda}$  and  $\rho_{\text{spec},\lambda}$  were weighted with the solar spectrum of ASTM G173-03 at air mass AM 1.5, which produced the solar weighted hemispherical reflectance  $\rho_{\text{SWH}}$  and the solar weighted specular reflectance  $\rho_{\text{SWS}}$  in the range from 250-2500nm.

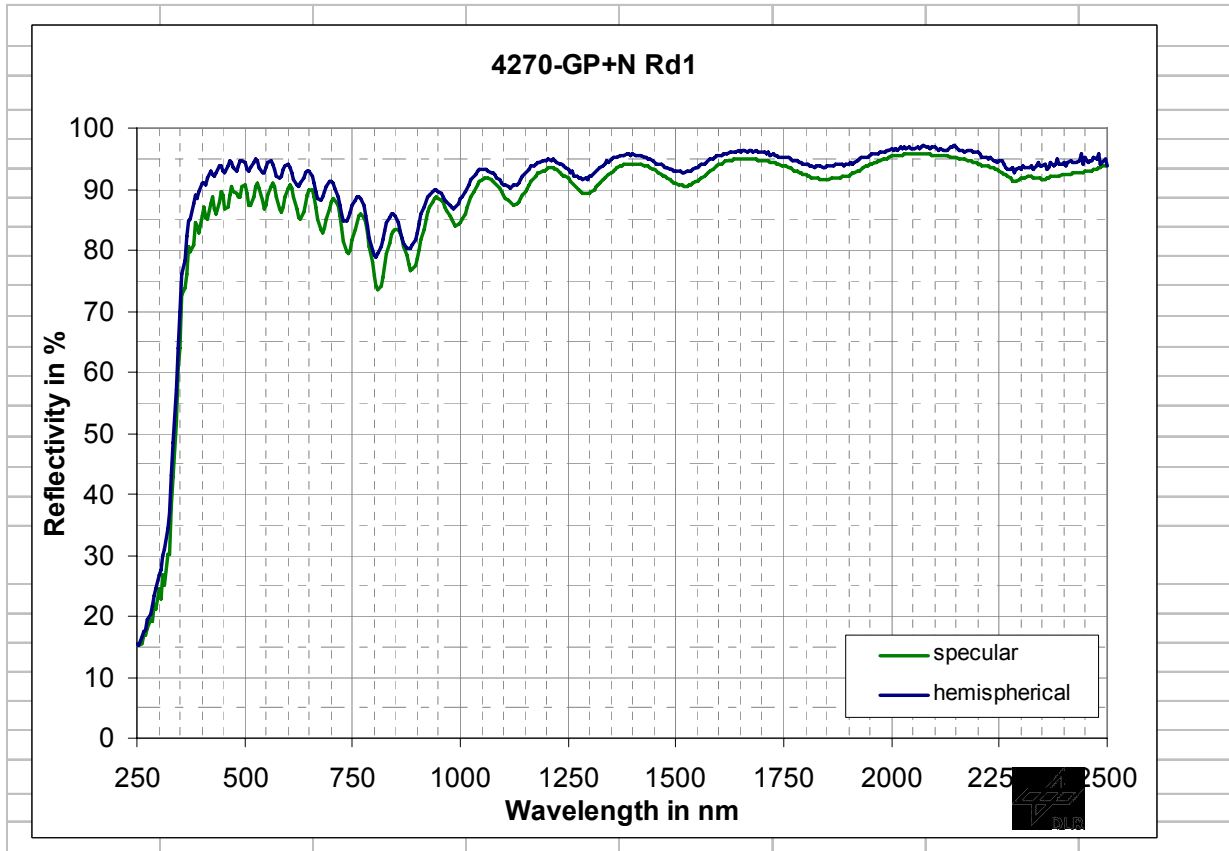
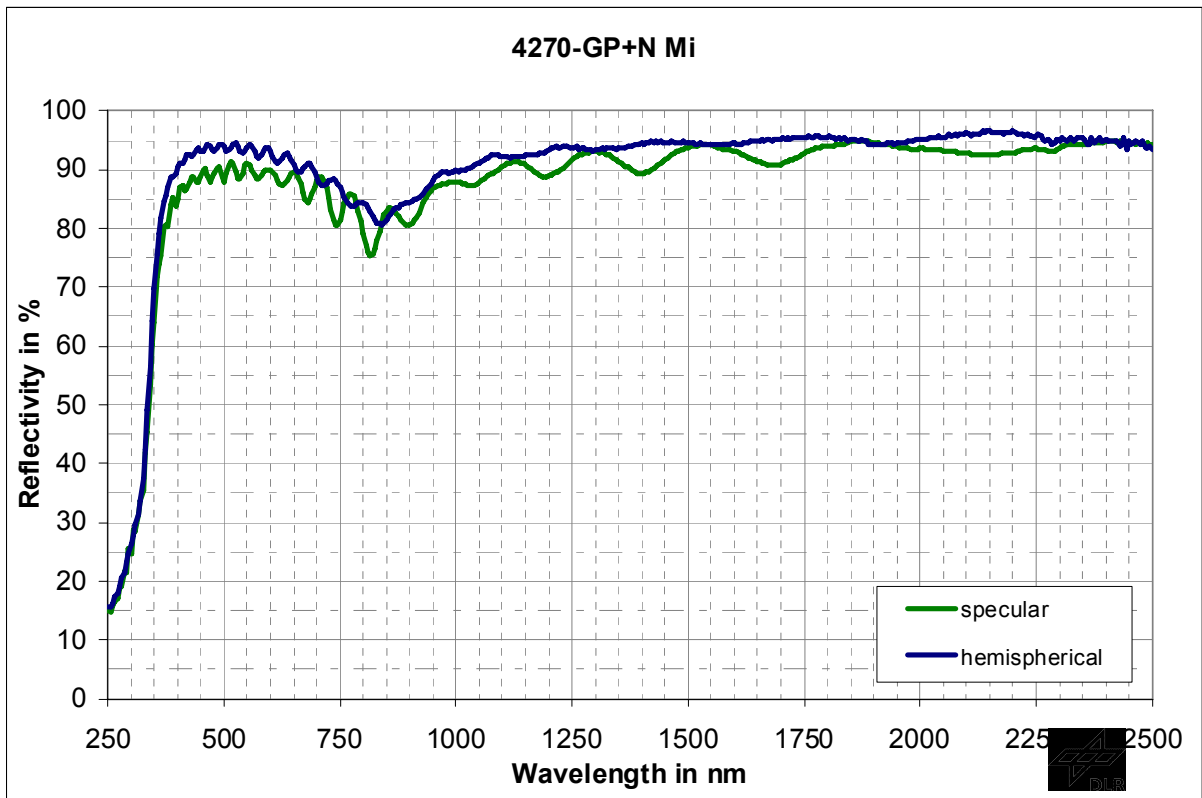
With a CCD-camera-assembly *Charm* an image of the specular reflected beam was taken. From the approximately Gaussian intensity distribution in the image, a deviation  $\sigma$  was determined and the associated half angle of diversion  $\alpha$  (angle to surface normal in mrad) was calculated. The average and standard deviation of the results of several measurements on different spots on the surface were taken.

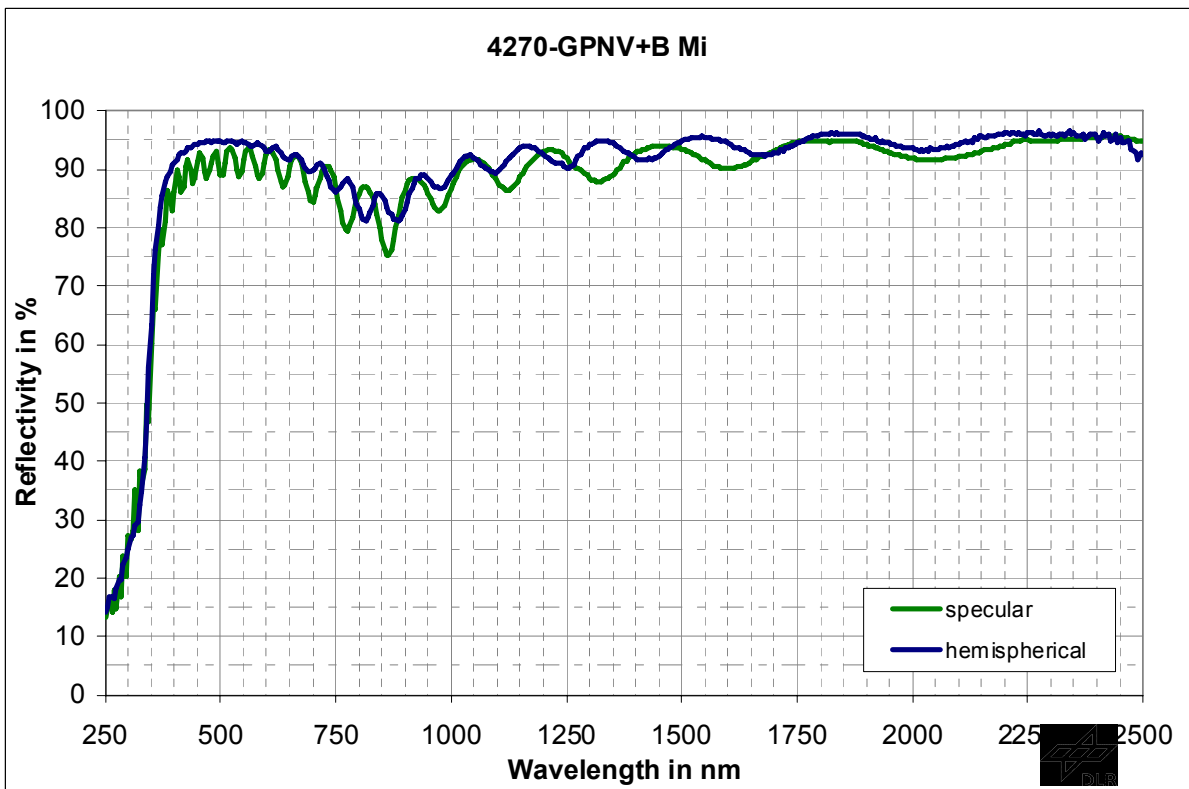
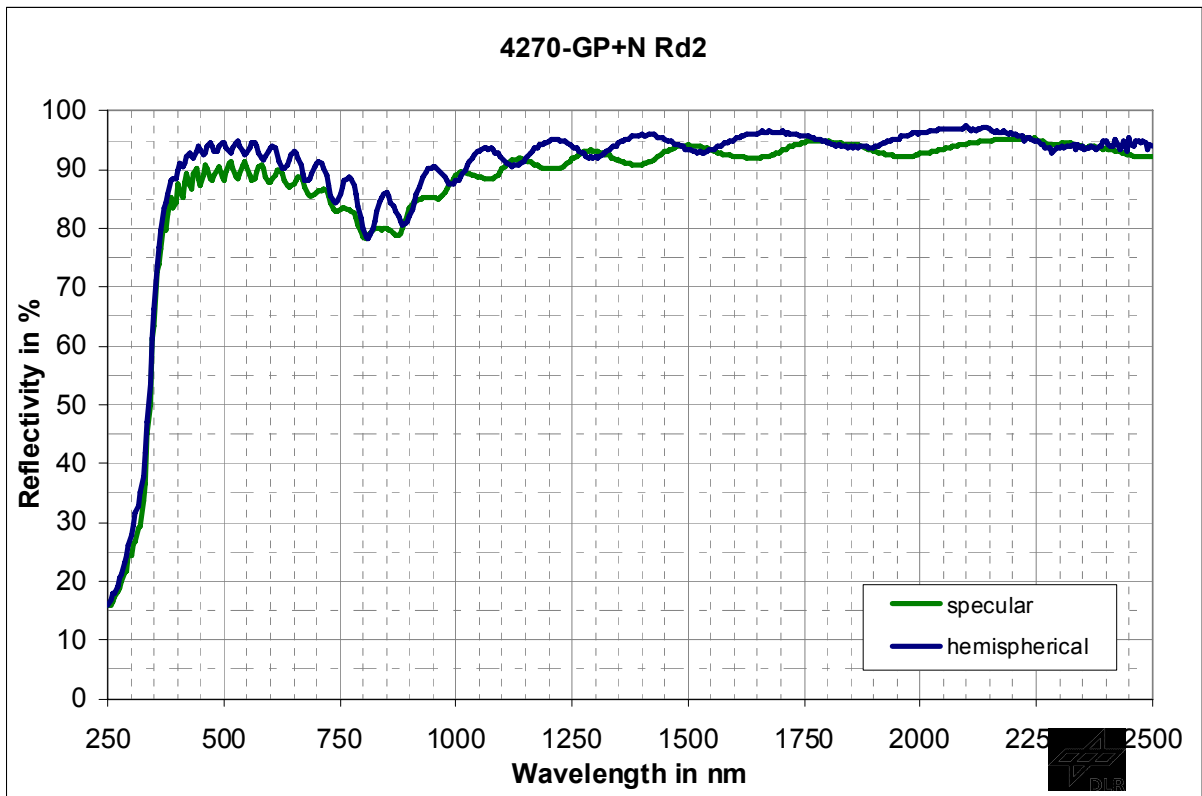
The samples are front reflecting aluminum mirrors, all except 4270 GP being coated with different kinds of varnish. All samples show longitudinal microstructures which are due to the rolling process. The surfaces are glossy and smooth, except for some local scratches. The coated samples show inhomogeneous color striae, with their characteristics depending on the varnish type. The distribution of those on the “GPNV + K-Lack” samples is mainly red and green and has the finest regional resolution. Color striae on “GPNV + B-Lack” samples are broader distributed and include yellow. Most inhomogeneous and very broad distributed are color striae in all colors on “GP + N-Lack” samples. Reflected images appear quite clear but are surrounded by a slight diffuse corona. The samples are sensitive to scratching. For the measurements parts of the samples were applied to an even glass substrate.

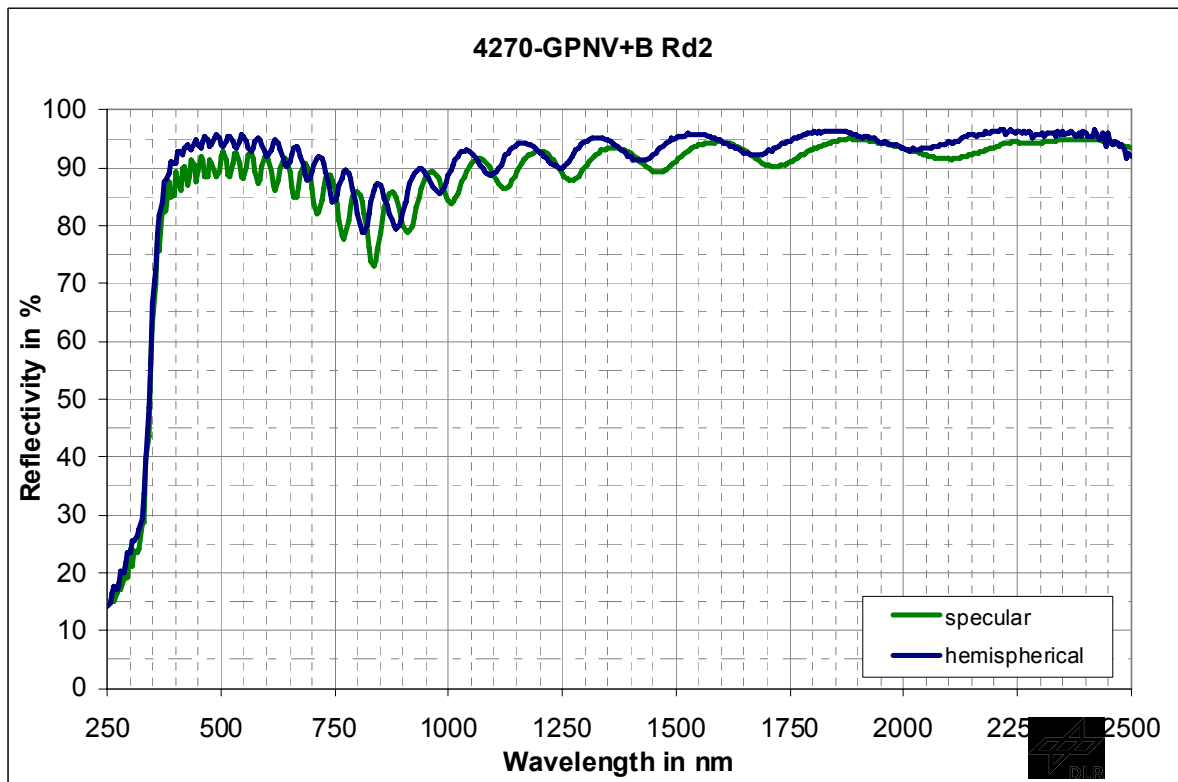
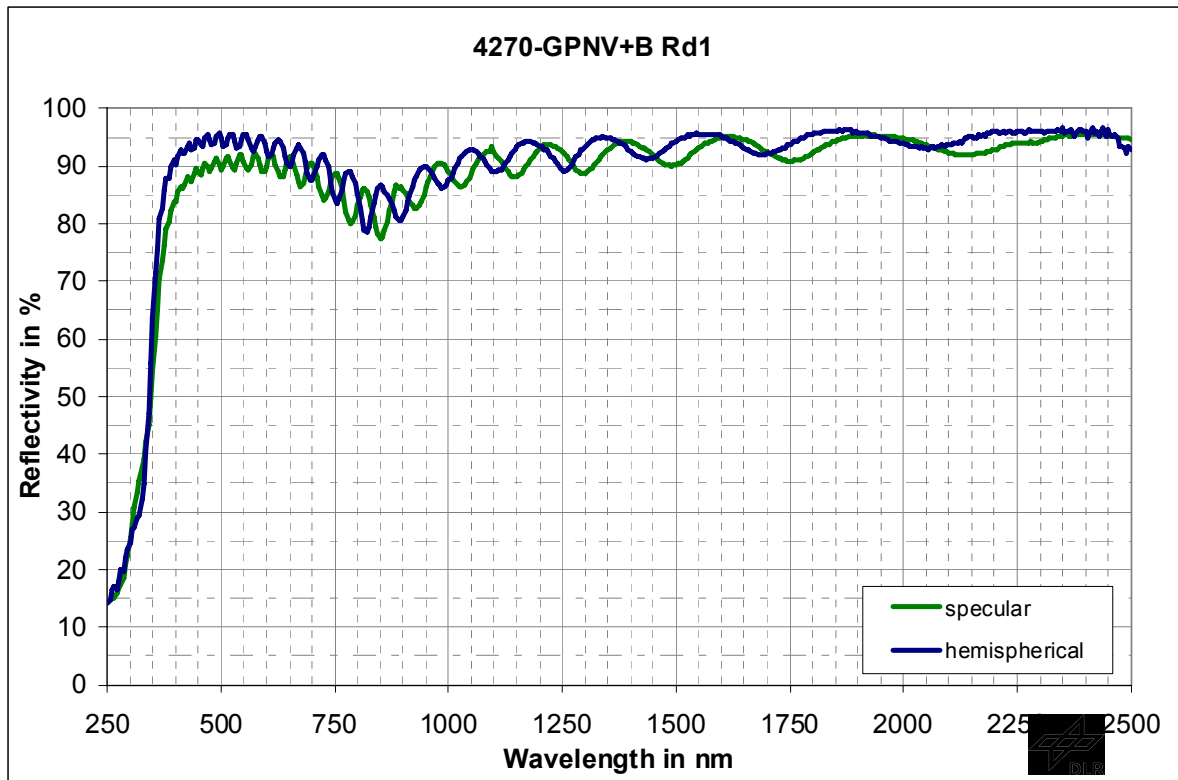
## 2. Results

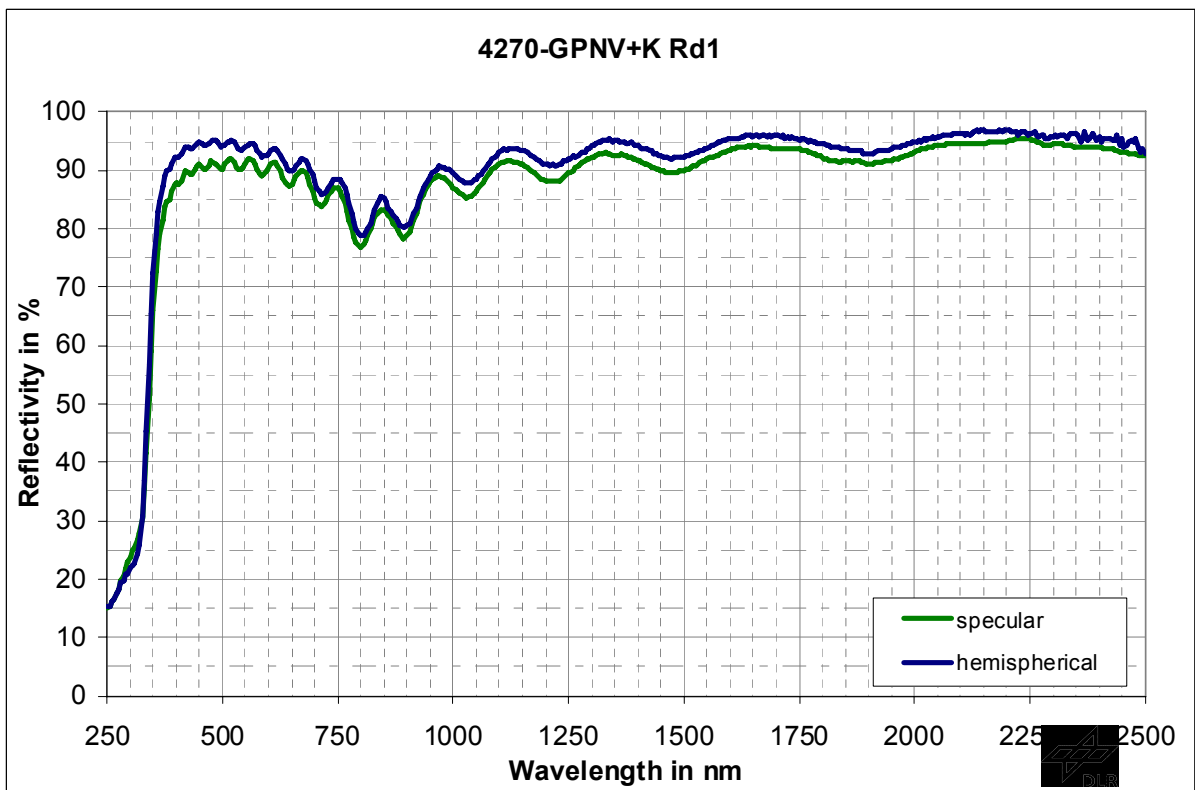
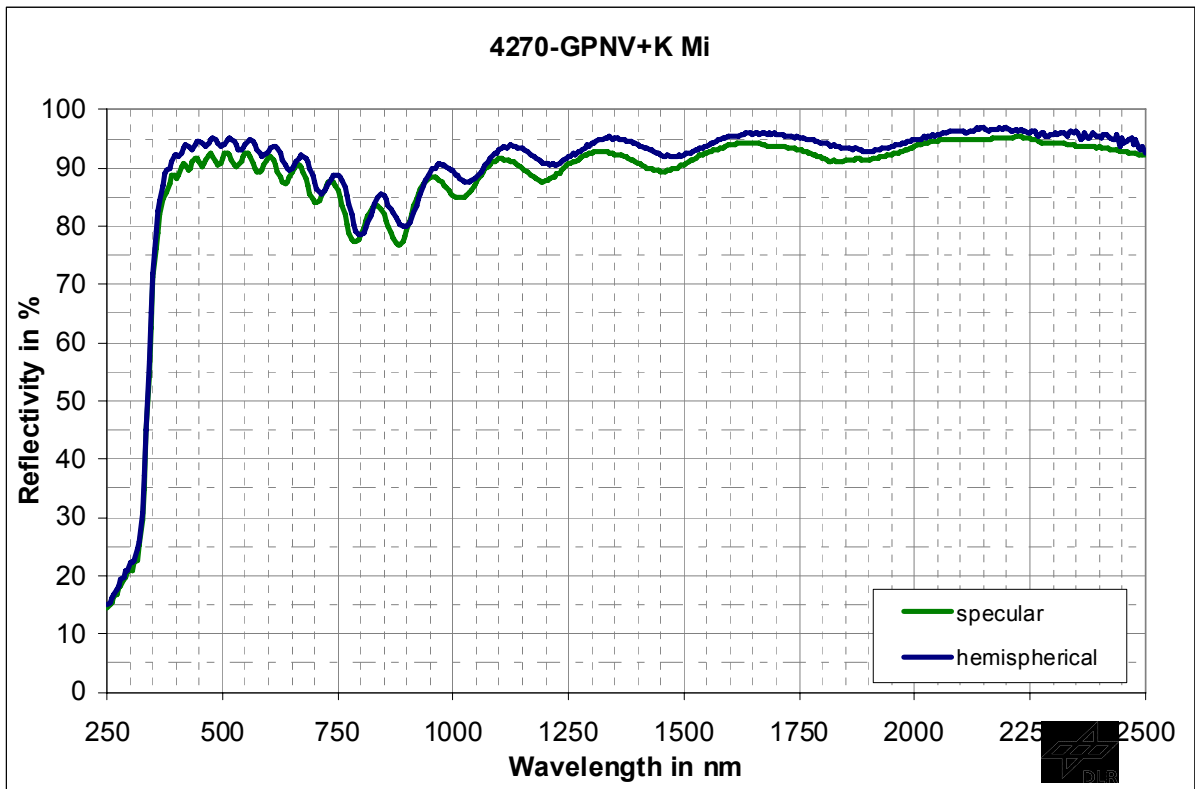
### 2.1. Averaged reflectance spectra

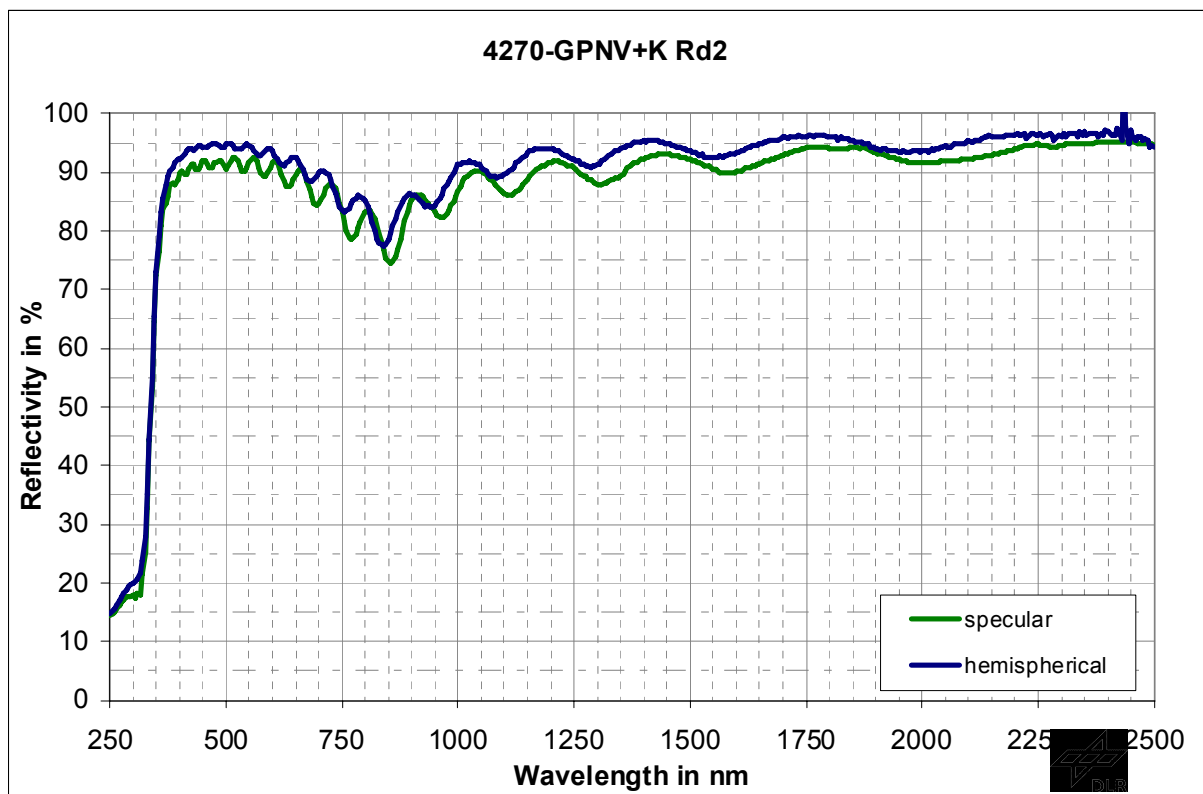












## 2.2. Calculated results

In Table 1 the numerical results are listed. The top columns display the mean reflectance taken from the hemispherical and specular spectra and weighted with the solar irradiance. Also, the specular beam diversion  $\alpha$  calculated from the images of chapter 2.3 is shown. Below that the results of the comparative calculations for gloss and reflectance losses are listed. Gloss represents the ratio of specular reflectance  $\rho_{SWS}$  to the hemispherical reflectance  $\rho_{SWH}$  and is dependent on the amount of light that is lost by scattering. A gloss value of 1 indicates no reflection losses due to scattering. This loss of reflectance is also quantified by subtraction and makes  $\Delta\rho_{SWH}-\rho_{SWS}$ . The results for gloss and subtraction-deltas are visualized in Figure 1 and the results of  $\alpha$  are visualized in Figure 2.

Sample	$\rho_{SWH}$	Stdv	$\rho_{SWS}$	Stdv	$\alpha$ [mrad]	Stdv [mrad]
GP Mi	<b>0,896</b>	0,04%	<b>0,875</b>	0,03%	<b>0,68</b>	0,07
GP-N Mi	<b>0,902</b>	0,05%	<b>0,872</b>	0,12%	<b>0,67</b>	0,33
GP-N Rd1	<b>0,902</b>	0,05%	<b>0,868</b>	0,12%	<b>1,20</b>	0,40
GP-N Rd2	<b>0,903</b>	0,12%	<b>0,873</b>	0,24%	<b>0,81</b>	0,35
GPNV-B Mi	<b>0,906</b>	0,14%	<b>0,883</b>	0,06%	<b>0,81</b>	0,29
GPNV-B Rd1	<b>0,906</b>	0,14%	<b>0,880</b>	0,09%	<b>0,99</b>	0,57
GPNV-B Rd2	<b>0,906</b>	0,12%	<b>0,875</b>	0,65%	<b>0,86</b>	0,74
GPNV-K Mi	<b>0,901</b>	0,12%	<b>0,878</b>	0,16%	<b>0,79</b>	0,19
GPNV-K Rd1	<b>0,901</b>	0,12%	<b>0,876</b>	0,08%	<b>0,81</b>	0,08
GPNV-K Rd2	<b>0,902</b>	0,08%	<b>0,877</b>	0,07%	<b>0,82</b>	0,18

Sample	Index	Gloss	$\Delta\rho_{SWH}$ - $\rho_{SWS}$
GP Mi	1	0,977	2,02%
GP-N Mi	2	0,966	3,03%
GP-N Rd1	3	0,962	3,40%
GP-N Rd2	4	0,967	3,02%
GPNV-B Mi	5	0,975	2,27%
GPNV-B Rd1	6	0,972	2,55%
GPNV-B Rd2	7	0,967	3,01%
GPNV-K Mi	8	0,975	2,26%
GPNV-K Rd1	9	0,973	2,44%
GPNV-K Rd2	10	0,972	2,57%

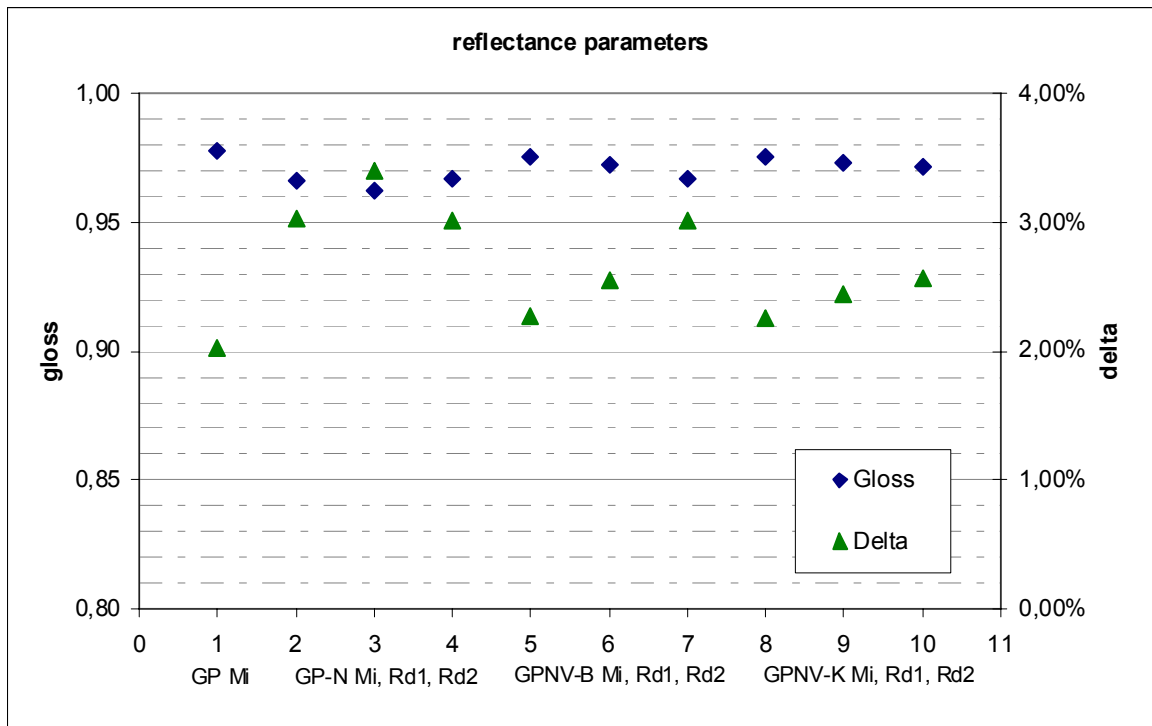


Figure 1

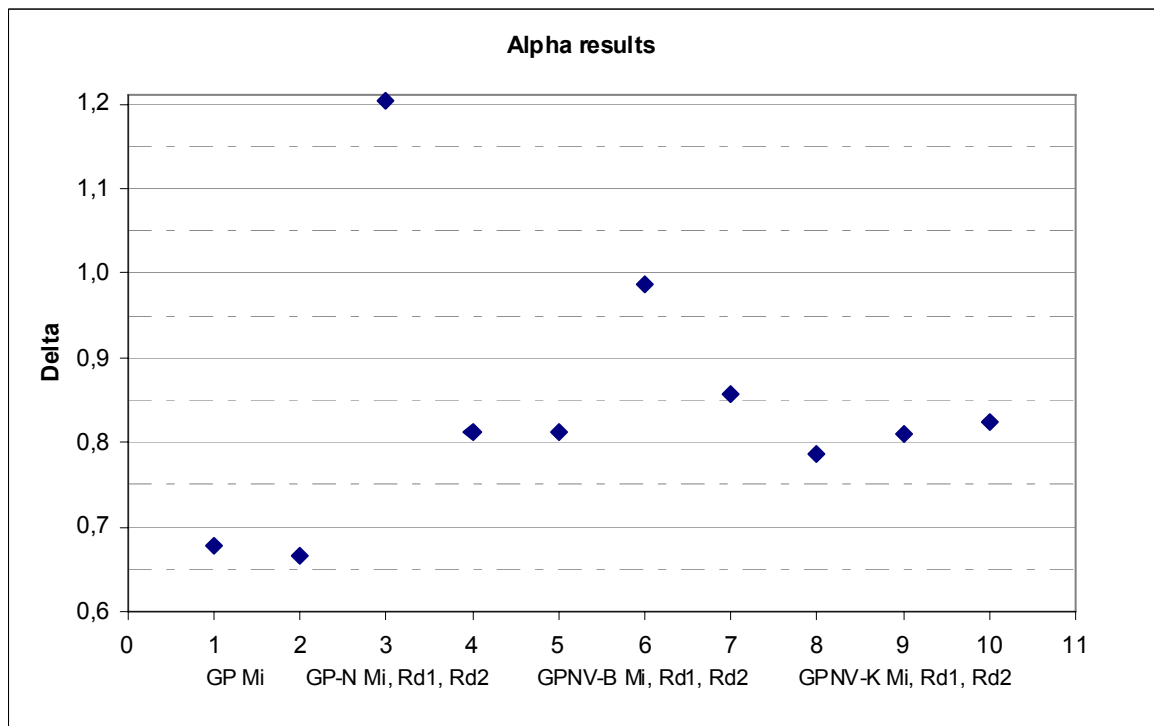
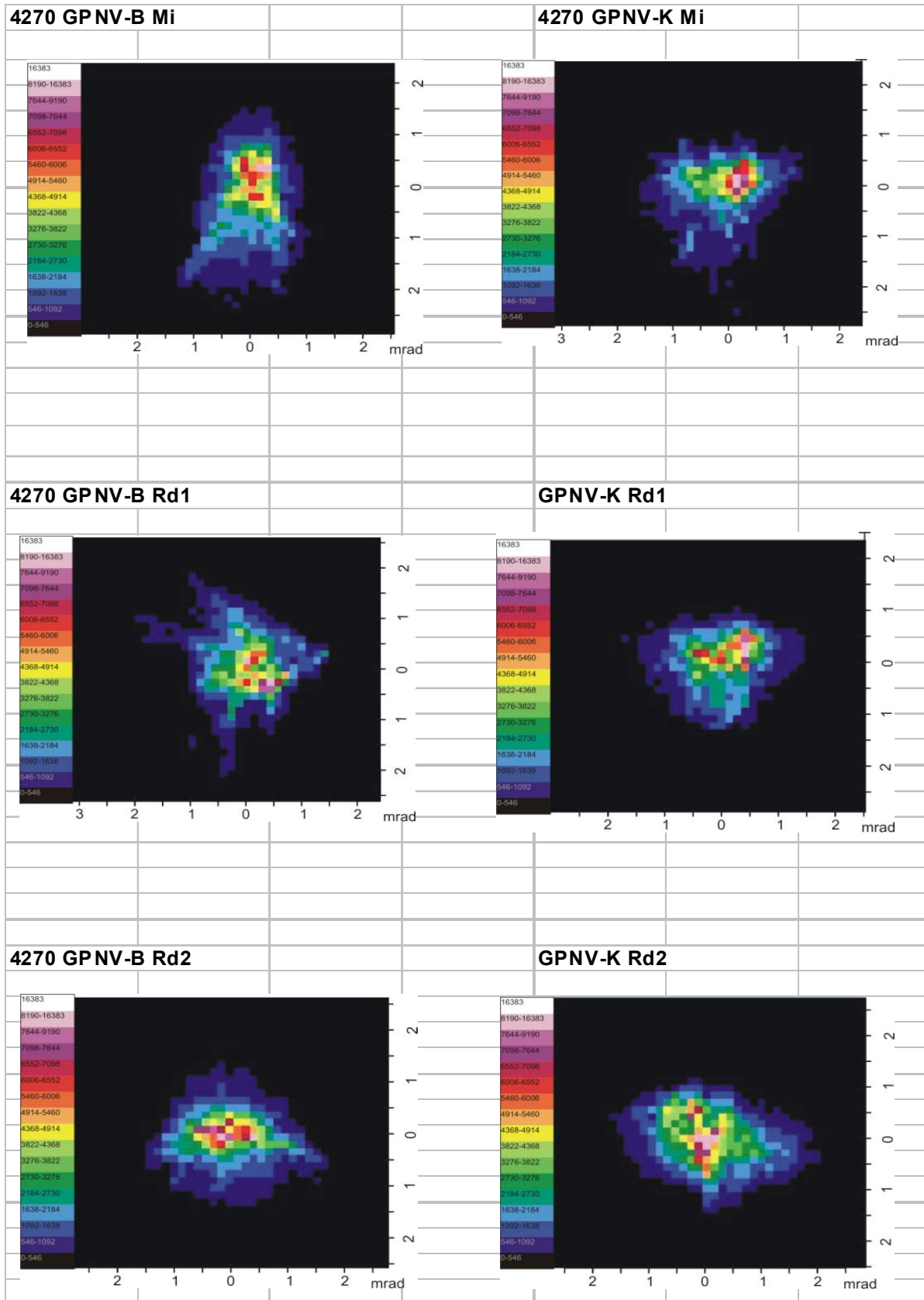
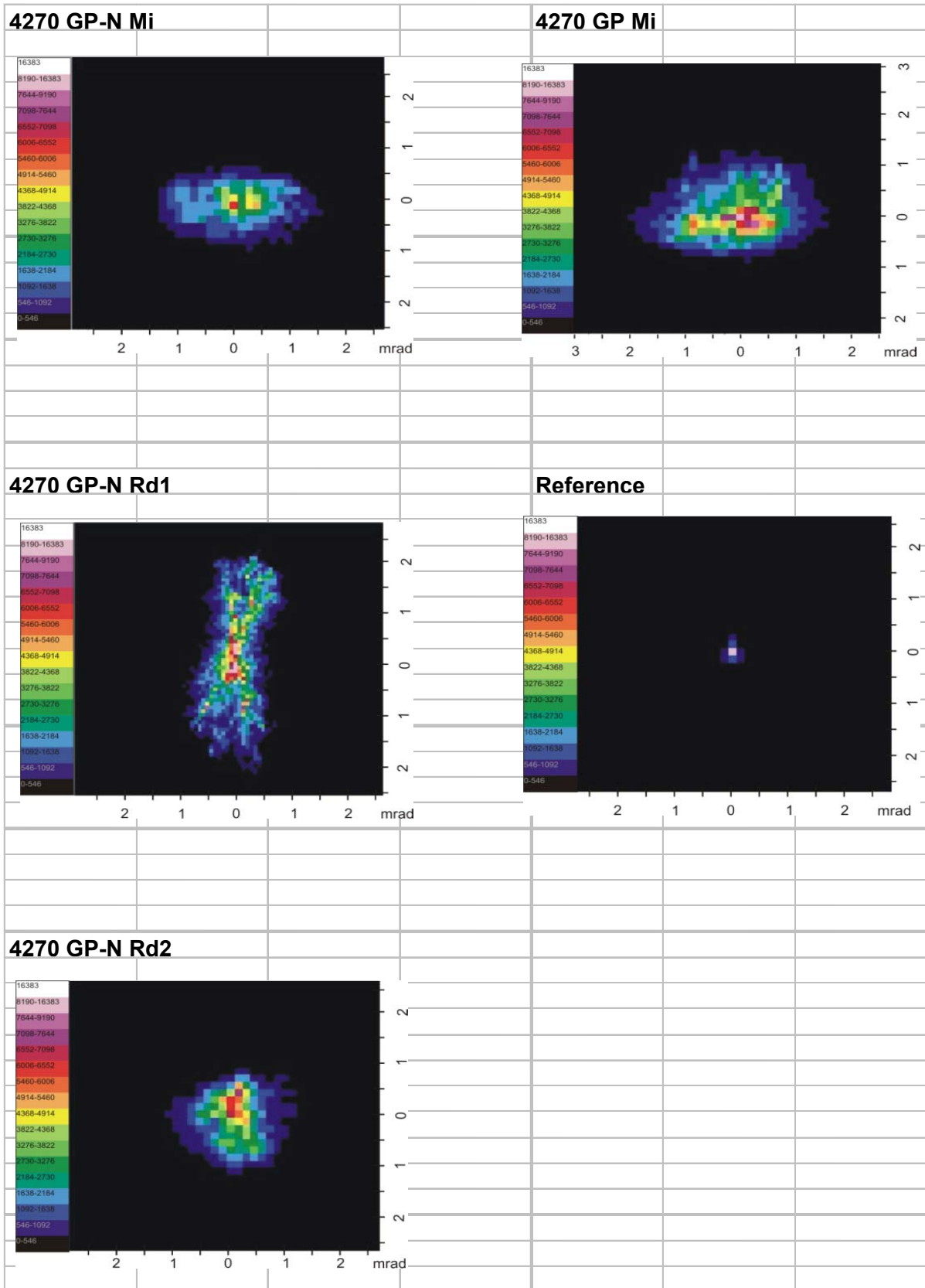


Figure 2

### 2.3. Images of specular beam diversion





### 3. Summary and evaluation

Ten samples from four different material-types provided by Alanod have been undertaken an optical reflection analysis. The spectral reflectance was measured with a *Perkin-Elmer Lambda 950* spectrometer, equipped with an *integrating sphere accessory* for hemispherical reflectance and a *universal reflectance accessory (URA)* for specular reflectance. Through convolution of the resulting data with the standard solar spectrum for air mass AM 1.5 the solar weighted hemispherical reflectance  $\rho_{\text{SWH}}$  and the solar weighted specular reflectance  $\rho_{\text{SWS}}$  were obtained. The latter value is important for application in CSP because it shows the amount of radiation that can be concentrated onto the absorber. The URA has an undefined acceptance angle for the reflected beam and has been used in substitution of the D&S reflectometer. The values of the D&S reflectometer measurements in aperture angles of 15, 25 and 46 mrad will be added to this report once they are available. The diversion of the specularly reflected beam was also measured with a camera assembly *Charm* and the half angle of diversion  $\alpha$  taken from  $1\sigma$  of the beam distribution was calculated.

A typical concentrating solar receiver has an acceptance angle range of 12-40 mrad depending on precision and concentration ratio, which requires a total beam quality ( $\sigma_{\text{total}}$  including all collector errors) of 7-16 mrad. The corresponding radius aim for the specular reflected beam is determined by a standard deviation of 2-4 mrad. The *Charm* measurements of the samples show, that the beam diversion is similar for all material samples, ranging from 0.67 to 1.20 mrad, which is not critical for concentrating solar applications.

The varnish applied on samples GP-N, GPNV-B and GPNV-K is responsible for interference effects that are either destructive or additive dependent on the wavelength. This becomes visible in the spectrum graphs and is a cause for the color striae. The peaks and valleys of the compared hemispherical and specular graphs are not constantly connected to certain wavelengths, probably because of local variations in the thickness of the top coating. This effect introduces a greater uncertainty in the comparison values.

The samples of "4270 GPNV + B-Lack" have the highest solar weighted hemispherical reflectance ( $\rho_{\text{SWH}} = 0.906$ ), while sample "4270 GP" without coating reaches the lowest values of 0.896. The others lie in the middle range. Considering the solar weighted specular reflectance  $\rho_{\text{SWS}}$ , "4270 GPNV + B-Lack" again reaches the highest values followed by "4270 GPNV + K-Lack". The surface scattering of the "4270 GP + N-Lack" samples is greatest, which is why there is a reflectance loss in relation to the hemispherical reflectance of over 3 percentage points. Apart from the reflectance value, sample "4270 GP" has the best overall reflection qualities with the highest gloss of 0.977 and the least loss to scattering of approx. 2 percentage points. The gloss of all samples varies between 0.966 and 0.977.

The measured samples show solar weighted specular reflectance values of 0.868 – 0.883 as measured with the *universal reflectance accessory (URA)* in the spectrometer. The optical analysis of the beam spread distribution shows that most of the reflected energy can be captured within a radius determined by a standard deviation of 0.67 – 1.20 mrad, corresponding to a target radius of 2-4 mrad. This shows that the analyzed materials can be used in such applications. This study has analyzed new material samples. The stability of these properties will depend on ambient conditions in the final applications.